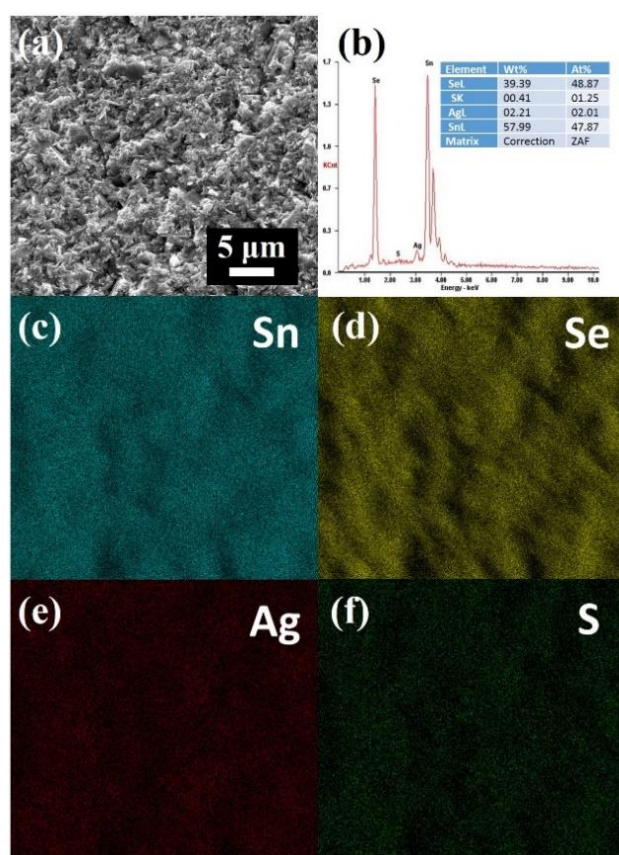


# Electronic Supplementary Information

## Independently Tuning the Power Factor and Thermal Conductivity of SnSe via Ag<sub>2</sub>S Addition and Nanostructuring

Yuanhu Zhu,<sup>a</sup> Jesús Carrete,<sup>b</sup> Qing-Long Meng,<sup>a</sup> Zhiwei Huang,<sup>a,d</sup>  
Natalio Mingo,<sup>c</sup> Peng Jiang,<sup>\*,a,d</sup> Xinhe Bao<sup>\*,a,d</sup>



**Fig. S1.** (a) SEM of SS1-Nano and (b)-(f) corresponding EDX elemental mapping.

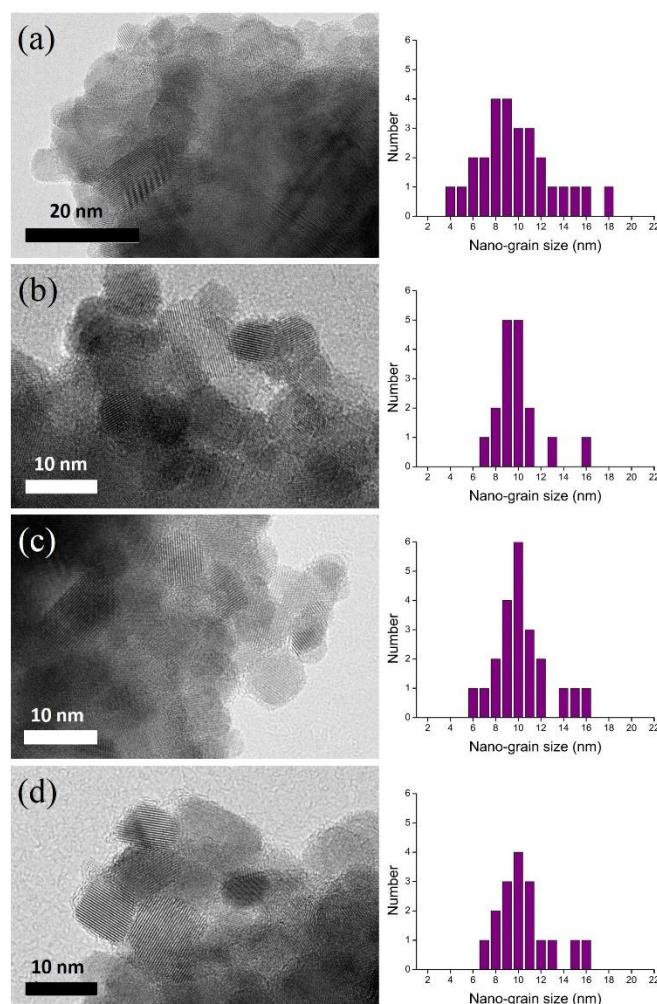


**Fig. S2.** TEM images and statistical distribution of nanograins in SS1-Nano.

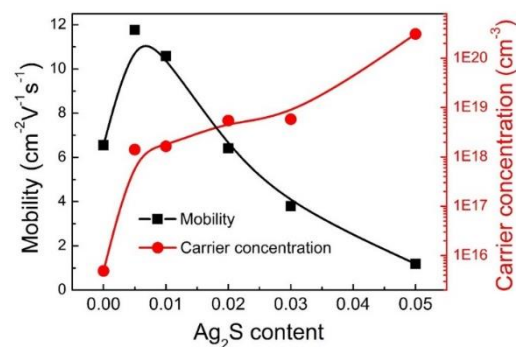


**Fig. S3.** Carrier concentration and mobility of SnSe+xAg<sub>2</sub>S (x = 0, 0.005, 0.01, 0.02, 0.03, 0.05) measured parallel to pressure direction at room temperature.

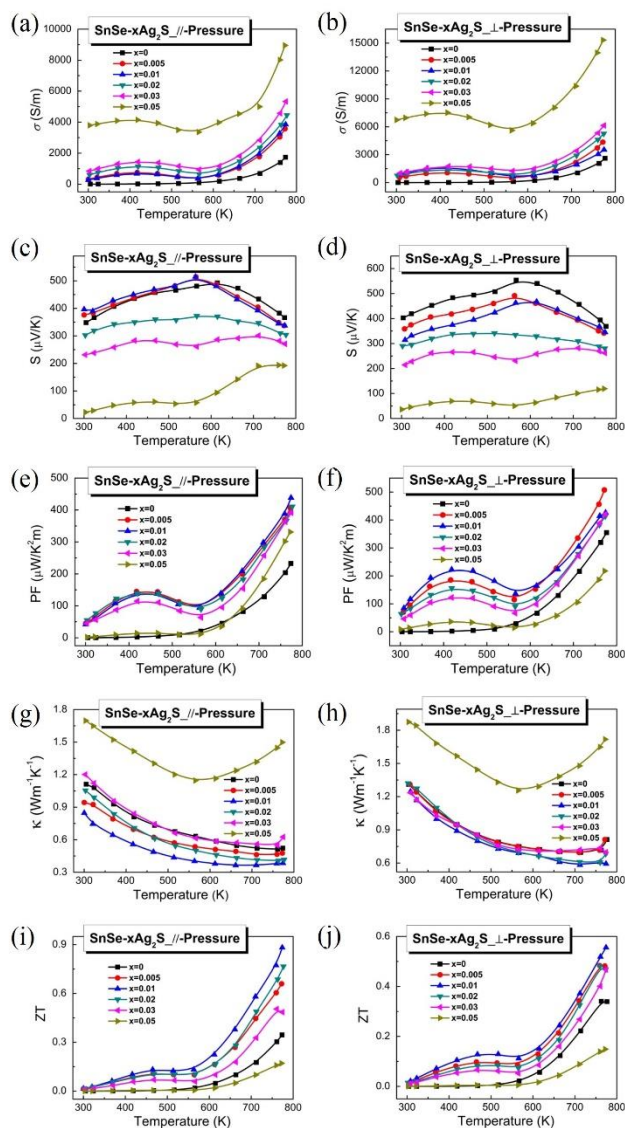


**Fig. S4.** Temperature dependence of electrical conductivities of SnSe+xAg<sub>2</sub>S ( $x = 0, 0.005, 0.01, 0.02, 0.03, 0.05$ ) (a) parallel and (b) perpendicular to pressure direction, (c)(d) Seebeck coefficients, (e)(f) power factors, (g)(h) thermal conductivities, and (i)(j) ZTs.

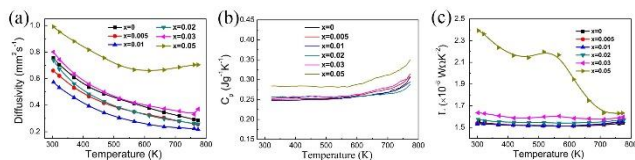


**Fig. S5.** (a) Diffusivity, (b) specific heat capacity, and (c) Lorenz number of SnSe+xAg<sub>2</sub>S ( $x = 0, 0.005, 0.01, 0.02, 0.03, 0.05$ ) parallel to pressure direction.

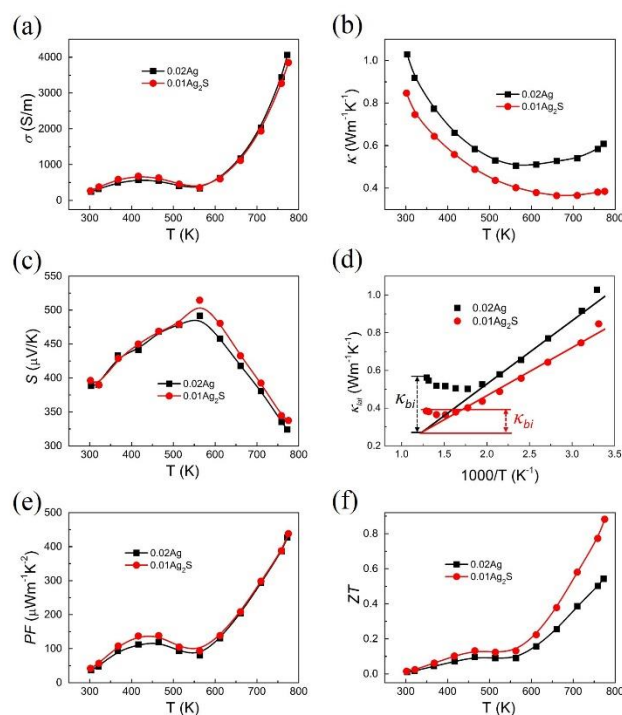


**Fig. S6.** Temperature dependence of (a) electrical conductivities, (b) Seebeck coefficients, (c) power factors, (d) total thermal conductivities, (e) lattice thermal conductivities and (f) ZTs for SnSe+0.02Ag and SnSe+0.01Ag<sub>2</sub>S.

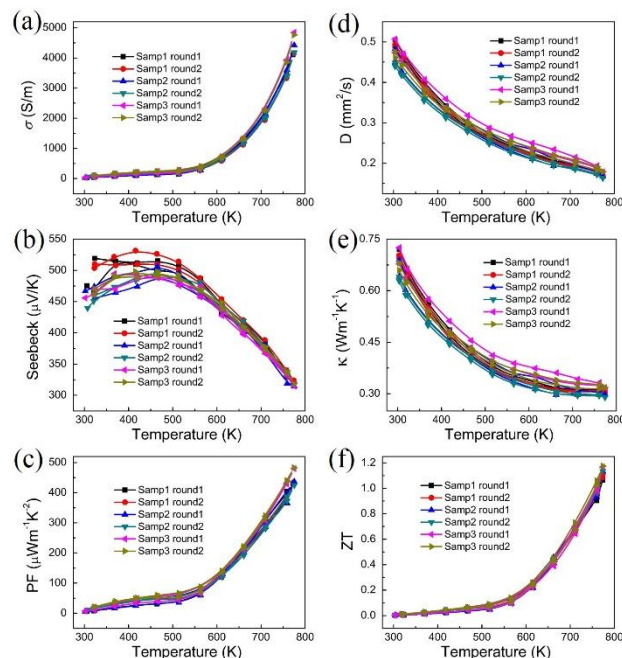


**Fig. S7.** Reproduced thermoelectric properties of the SS1-Nano samples while both heating and cooling: (a) electrical conductivities, (b) Seebeck coefficients, (c) power factors, (d) diffusivities, (e) total thermal conductivities, and (f) ZTs.

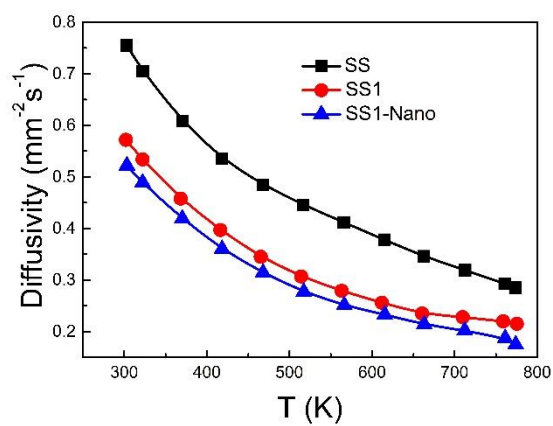


**Fig. S8.** Temperature dependence of diffusivities for SS, SS1, SS1-Nano.